Behavioural Brain Research 408 (2021) 113285

Contents lists available at ScienceDirect

Behavioural Brain Research

journal homepage: www.elsevier.com/locate/bbr

Recognition memory performance can be estimated based on brain activation networks

Jana Petrovska [a,c,*], Eva Loos [b,c], David Coynel [b,c], Tobias Egli [a,c], Andreas Papassotiropoulos [a,c,d,e], Dominique J.-F. de Quervain [b,c,d], Annette Milnik [a,c,d,*]

[a] Division of Molecular Neuroscience, Department of Psychology, University of Basel, CH-4055 Basel, Switzerland
[b] Division of Cognitive Neuroscience, Department of Psychology, University of Basel, CH-4055 Basel, Switzerland
[c] Transfaculty Research Platform Molecular and Cognitive Neurosciences, University of Basel, CH-4055 Basel, Switzerland
[d] Psychiatric University Clinics, University of Basel, CH-4055 Basel, Switzerland
[e] Department Biozentrum, Life Sciences Training Facility, University of Basel, CH-4056 Basel, Switzerland

ARTICLE INFO

Keywords:
fMRI
Independent component analysis (ICA)
Recognition
Memory
Prediction

ABSTRACT

Background: Recognition memory is an essential ability for functioning in everyday life. Establishing robust brain networks linked to recognition memory performance can help to understand the neural basis of recognition memory itself and the interindividual differences in recognition memory performance.
Methods: We analysed behavioural and whole-brain fMRI data from 1′410 healthy young adults during the testing phase of a picture-recognition task. Using independent component analysis (ICA), we decomposed the fMRI contrast for previously seen vs. new (old-new) pictures into networks of brain activity. This was done in two independent samples (training sample: $N = 645$, replication sample: $N = 665$). Next, we investigated the relationship between the identified brain networks and interindividual differences in recognition memory performance by conducting a prediction analysis. We estimated the prediction accuracy in a third independent sample (test sample: $N = 100$).
Results: We identified 12 robust and replicable brain networks using two independent samples. Based on the activity of those networks we could successfully estimate interindividual differences in recognition memory performance with high accuracy in a third independent sample ($r = 0.5$, $p = 1.29 \times 10^{-07}$).
Conclusion: Given the robustness of the ICA decomposition as well as the high prediction estimate, the identified brain networks may be considered as potential biomarkers of recognition memory performance in healthy young adults and can be further investigated in the context of health and disease.

1. Introduction

Recognition memory describes the ability to judge whether an object or event has been previously encountered [1]. This ability is essential for functioning in everyday life and has an important role in shaping one's future behaviour and decision making [2,3]. Thus, recognition memory paradigms are widely used in empirical research on human cognition in both health and disease [4–6]. One of the most commonly applied methods for recognition memory investigation is the Remember-Know (R-K) paradigm [7,8]. The R-K paradigm estimates recognition memory based on familiarity, typically defined as a general sense of knowing, and recollection, defined as remembering specific details associated with the recognised object or event [4]. An alternative view is that recollection and familiarity are not distinct processes but rather describe differences in memory strength (high and low, respectively) [9].

Based on fMRI studies using task-based contrasts, recognition memory processes have been linked to activation in multiple brain regions, such as the (para)hippocampus and perirhinal cortex in the medial temporal lobe, parts of the prefrontal cortex (PFC), the thalamus and the parietal cortex [10–18]. Importantly, using different recognition memory contrasts facilitates the identification of brain regions that are specifically involved in the distinct sub-processes of recognition memory. For example, the anterior and posterior midline cortex, the angular gyrus, and medial temporal regions of the default mode network (DMN) emerge in the recalled > familiar contrast, the dorsal frontal and parietal cortices of the dorsal network emerge in the familiar > recalled contrast

* Corresponding authors at: University of Basel, Divisions of Molecular Neuroscience, Birmannsgasse 8, CH-4009 Basel, Switzerland.
E-mail addresses: jana.petrovska@unibas.ch (J. Petrovska), annette.milnik@unibas.ch (A. Milnik).

https://doi.org/10.1016/j.bbr.2021.113285
Received 2 November 2020; Received in revised form 11 March 2021; Accepted 30 March 2021
Available online 2 April 2021

and the ventral frontal and parietal cortices, the insular cortex, and the caudate regions of the ventral network emerge in a contrast based on increasing familiarity strength or confidence [18]. Based on such contrasts, distinct brain activation patterns have been detected for familiarity-based vs. recollection-based recognition memory across the medial temporal lobe, frontal, parietal and sensory cortices and subcortical areas [11,15].

These contrast-based analyses allow the identification of regions that are in general more (or less) active during a task or in a specific condition. However, they rarely make inferences about interindividual differences in the behavioural outcome. Of note, a recognition memory study has shown that brain activation of specific regions of interest (ROIs) within a core recollection network, including the medial PFC and the right hippocampus, is additionally associated with interindividual differences in task performance [19].

Instead of using task-based contrasts and ROI approaches to investigate the link between brain activation and behaviour, more sophisticated network-level analyses can be used not only to identify large-scale brain networks but also to investigate their impact on individual differences in task performance [20,21]. These analyses identify brain networks as the joint co-dependent activity of different parts of the brain [20]. It has been already shown that widespread functional brain networks are recruited by diverse behavioural tasks, as well as during rest [22–24].

Functional connectivity approaches have been successfully applied in the context of episodic memory performance [25,26]. Schedlbauer et al. demonstrated that higher connectivity in key regions like the hippocampus, prefrontal cortex, precuneus and visual cortex is related to successful memory retrieval [26]. King et al. showed that recollection-dependent wide-spread functional connectivity of seed regions within a core recollection network comprising the angular gyrus, the medial prefrontal cortex, the hippocampus, the middle temporal gyrus and the posterior cingulate cortex is associated with recollection performance on three behavioural tasks, including the R-K paradigm [25]. Furthermore, recent studies have linked network-level brain activation to memory-related behavioural outcomes, including working memory performance, emotional memory and recollection speed of a context memory, using purely data-driven voxel-wise dimensionality reduction techniques [27–29].

Utilizing such a network-level approach may lead to a more comprehensive picture of the neural bases of recognition memory and their impact on interindividual differences in memory performance. Therefore, we applied a whole-brain, data-driven dimensionality reduction approach to identify brain networks related to the testing phase of a recognition memory task and investigated their relationship with interindividual differences in participants' overall task performance, as well as in familiarity and recollection separately. We used fMRI data from 1′410 healthy young adults who had performed a picture-recognition task in the MRI scanner. The large number of participants allowed us to identify robust and replicable brain networks. Additionally, it enabled us to perform prediction analysis instead of simple association analysis, which allows for a higher generalizability of our results [30,31].

2. Materials and methods

2.1. Study design

Healthy young adults took part in a large-scale, single-centre fMRI study in Basel, Switzerland, conducted between 2008 and 2015. The study has been described elsewhere [27,32,33]. Participants were free of any medication other than oral contraceptives and of any neurological and psychiatric illness at the time of the study. All participants provided written informed consent prior to study participation. The study protocol was approved by the ethics committee of the Cantons of Basel-Stadt and Basel-Landschaft.

2.2. Description of picture encoding and picture recognition task

1′446 participants performed a picture encoding task for 20 min. They were shown 72 meaningful pictures of positive, negative and neutral valence (24 per emotional valence category), and 24 scrambled pictures. Two additional neutral pictures were presented at the beginning and two at the end of the picture-encoding task, in order to account for potential primacy and recency effects. Each picture was presented for 2.5 s in a quasi-randomised order (no more than four consecutive pictures per category). A 500 ms fixation-cross appeared before each picture presentation. Each picture was rated on two separate three-point Likert scales, measuring subjective arousal and valence of positive, negative and neutral pictures and form and size of scrambled pictures. Ratings were given via button presses with three fingers of the participant's preferred hand. Immediately after picture encoding, participants performed an N-Back task for 10 min, serving as a distractor task between picture encoding and testing. For a detailed description of the N-Back task please see [27]. Subsequently, an unannounced free recall task was performed outside the scanner without a time limit.

The picture recognition task took place approximately 80 min after the picture encoding task and lasted for 20 min. Participants were presented with the 72 old pictures shown in the encoding task and a set of new pictures comprising again 72 meaningful pictures with positive, negative and neutral valence (24 per emotional valence category). Pictures were presented in a quasi-randomised order (no more than 4 consecutive pictures per category). A 500 ms fixation-cross appeared before each picture presentation. Participants subjectively rated each picture as remembered, familiar or new on a three-point Likert scale within 3 s after picture presentation via button presses with three fingers of their preferred hand. Participants were instructed to rate a picture as remembered if they were certain that they have seen it during the encoding phase of the experiment that took place in the scanner. If they were not certain that they saw the specific picture in the scanner, or only had a feeling of "déjà vu" for the picture, they were instructed to rate it as familiar. Participants rated pictures as new if they were certain that they have never seen them before. The picture recognition task was followed by 20 min of structural MRI (T1) and DTI acquisition. The complete experiment lasted 3–4.5 h per participant. Participants were compensated with 25 CHF/h.

For the encoding and the picture recognition task we used pictures from the International Affective Picture System (IAPS) [34]. The neutral pictures were additionally complemented by 8 in-house standardised pictures to equate for visual complexity and content of the stimuli.

We estimated the recognition memory performance of old and new pictures by calculating false-alarm corrected performance scores separately for familiarity (number of old pictures rated as "familiar" – number of new pictures rated as "familiar") and for recollection (number of old pictures rated as "recalled" – number of new pictures rated as "recalled"). We then calculated the overall recognition memory performance as the sum of false-alarm corrected familiarity scores and false-alarm corrected recollection scores.

2.3. Subsampling

In order to obtain independent samples needed for the subsequent analyses (building of independent brain networks and prediction analysis), we divided our full sample of $N = 1'446$ participants with complete behavioural data in three samples. We created two equally sized samples ($N = 673$ participants) and an additional sample of $N = 100$ participants, referred to as training, replication and test sample throughout the paper. The samples were created by chronologically ordering the participants and then performing the sample split.

2.4. (f)MRI data acquisition, preprocessing and first-level analysis

Siemens Magnetom Verio 3 T whole-body MR unit equipped with a

twelve-channel head coil was used for scanning. (f)MRI data acquisition, preprocessing and the construction of a population-based anatomical probabilistic atlas have been described elsewhere [27] and are also reported in the Supplementary Information. Preprocessing and first-level analysis of the fMRI data was performed using the software SPM8 (Statistical Parametric Mapping, Wellcome Trust Centre for Neuroimaging; http://www.fil.ion.ucl.ac.uk/spm/) in MATLAB R2012b (MathWorks) using a standard fMRI pipeline.

Brain activation during presentation of old (previously presented during the encoding task) and new (not previously presented) pictures during the testing phase of the recognition task was separately estimated per participant.

The difference between the old and the new picture parameter estimates was calculated for each participant and voxel (first-level analysis for old-new contrast). Performance measurements were not included in the analysis.

2.5. fMRI second-level analysis

All further analyses were conducted with the statistical software R (3.4.2; RRID:SCR_001905). The old-new contrast parameters were included in a second-level group analysis. Only participants with complete fMRI data (training sample: $N = 648$; replication sample: $N = 665$; test sample: $N = 100$) were included. Additionally, we removed participants with missing values for > 10 % of voxels ($N = 3$ in the training sample) and voxels with any missing values ($N = 14'458$). The final sample included 1′410 participants (training sample: $N = 645$; replication sample: $N = 665$; test sample: $N = 100$) and 56′764 voxels.

We regressed out the effects of age and sex from the voxel signal separately for the training and the replication sample and used the scaled residuals in all subsequent analyses. Scanner-related confounding variables (gradient coils and software changes) were present in the training sample and were also regressed out. To achieve independence on participant level in the test sample for the prediction analysis, we corrected for sex and age by applying the sex and age beta values derived from the training sample to the test sample. Scaling in the test sample was also based on the parameter derived from the training sample.

2.6. Identification of independent brain networks using ICA decomposition

We used ICA in order to decompose the whole-brain fMRI signal into a set of voxel-wise independent components. ICA is a dimensionality reduction method used for linear representation of non-Gaussian data by decomposing them into components that are as statistically independent as possible [35]. We applied ICA to a matrix X (old-new contrast parameters), comprising m observations (participants) and n variables (voxels). ICA estimates a matrix of k x n latent sources S that underlie the variables, while holding the source estimates (voxel loadings) as independent from each other as possible. Therefore, by applying ICA decomposition to old-new contrast parameters (a matrix with participants as rows and voxels as columns) our voxel loadings describe statistically independent latent sources that underlie the contrast estimates. Additionally, ICA provides a matrix of m x k mixing coefficients A (participants scores) for each independent component. The mixing coefficients of each component represent the component's activity strength, per participant [36]. Participants with high contrast estimates in voxels that load highly onto a particular component in a positive direction are assigned elevated scores for that component by this method. Therefore, we interpret the participants' scores as a measure of coactivation in the voxels that load onto the component.

2.7. Determining the optimal number of components

The number of independent components is a key ICA parameter, and there are several methods for its optimisation, such as estimation of component stability and reproducibility for ICA solutions with N number of components (ICA_N) [37,38], described in the following section.

2.7.1. ICA decomposition stability assessment

As a first step for identifying the optimal number of components for decomposition of the old-new fMRI contrast, we investigate the stability of decomposing the voxel signal into $N = 3$:24, 26, 28, 30 and 32 ICs (26 different ICA solutions: ICA_3 … ICA_{32}).

Procedure: 1) We used a resampling method with 100 repetitions and 90 % of randomly selected participants from the training sample, producing 100 similar, but non-identical subsamples, in order to prevent overfitting. 2) For each of the 26 ICA solutions: a) We performed ICA on each of the 100 subsamples, using the fastICA algorithm (R-package "fastICA"; [35]); b) We calculated the stability of each IC by applying Pearson's correlation to its voxel loadings across subsamples. Since the order of components derived from ICA is arbitrary (e.g. IC1 in one sample may be IC2 in another sample), we identified the corresponding components between our subsamples as the ones with the highest correlation across the subsamples. As the direction of IC estimates is also arbitrary, we squared the correlation coefficients to adjust for directionality (r^2); c) a given ICA solution stability was calculated as the mean stability of its ICs.

2.7.2. ICA decomposition reproducibility assessment

As a second step for identifying the optimal number of components, we investigated the reproducibility of the five most stable ICA solutions between the training and the replication sample. We limited the testing to the top five most stable ones in order to keep only ICAs with rather high stability and high reproducibility. For each ICA solution, we 1) conducted ICA with the complete training and replication sample, respectively (no subsampling), 2) created a correlation matrix by calculating Pearson's correlations between the voxel loadings per IC across samples. As the direction of IC estimates is arbitrary, we squared the correlation coefficients to adjust for directionality (r^2). Since the order of components derived from ICA is arbitrary, we reordered the replication sample ICs, so that each IC matches its corresponding training sample IC ($r^2 \geq 0.6$). Furthermore, as the direction of IC estimates is also arbitrary, we recoded IC estimates (voxels loadings and participants scores, respectively), so that estimates have the same direction in the training and replication sample and voxels with the highest absolute loadings have positive loadings.

From the correlation matrix for each ICA solution we estimated the average correlation coefficient on the diagonal, i.e., for matched ICs (X) and off the diagonal, i.e., for unmatched ICs (Y), across samples. We used mean(r^2_X) – mean(r^2_Y) as a reproducibility metric (Suppl. Fig. 2). The most reproducible ICA solution was used for all subsequent analyses. By doing so, we did not account for model sparsity, but solely focused on stability and reproducibility.

2.8. Recognition memory prediction

We built our prediction model based on the training sample ($N = 645$). Specifically, we performed one multiple linear regression model using the participants IC scores as predictors and recognition memory performance as the outcome variable.

We first estimated the model fit based on independently estimated ICs in the replication sample ($N = 665$). We applied the regression weights of the predictive model to the participants IC scores from the replication sample ICs.

Next, we estimated the model fit in the test sample ($N = 100$). Since ICA was not applied to the test sample, we projected the voxel loadings from the ICs in the training sample onto the old-new contrast parameters from the test sample, using the 'ginv' function from the R package "MASS" [39]. Using projected values enabled us to apply our model on the fMRI data from a new sample without subjecting it to ICA. Therefore, the model can also be applied on a single participant.

The model's accuracy for each sample was assessed by comparing the predicted behavioural outcome with the observed behaviour using Pearson's correlation (r). Statistical test for significance was done with a t-test (p-value threshold $< .05$).

Additionally, the described prediction analyses were conducted two more times, for familiarity-based and recollection-based recognition memory scores as the outcome variable, separately. The procedure for these analyses was identical to the one using the overall recognition memory scores.

2.9. Post hoc analyses

2.9.1. Reduction of the prediction model

Next, we investigated if a comparable prediction of the behavioural measures can be achieved by using a prediction model based on a reduced number of ICs, namely on the ones with the highest contribution to behaviour. In order to identify the most relevant ICs for each behavioural measure, we applied both forward and backward stepwise model selection using the "stepAIC" function from the "MASS" R package [39]. We used this function to select the best-performing model out of 13 possible linear models with 0–12 ICs as predictors and recognition memory as the dependent variable in the training sample. We then used the best-performing model in order to predict recognition memory performance in the replication and the test sample, respectively. The same procedure was repeated for familiarity and recollection performance, separately.

2.9.2. ICs association with performance on additional behavioural tasks

We conducted additional exploratory analyses to investigate the link between IC scores and the performance in behavioural tasks conducted at a different time point. Specifically, we applied a multiple linear regression model using the participants' IC scores as independent variables and different memory-related behaviours as the outcome variable in the training, replication and test sample, respectively. This analysis was conducted for two different behavioural measures, separately: A) Participants' performance on the unannounced picture free-recall task outside of the MRI scanner, calculated as the total number of correctly remembered pictures; B) Participants' performance on a N-Back task conducted in the MRI scanner, calculated as a D-prime measure [40] for the 2-Back condition. Both the N-Back task and the picture free-recall were performed prior to the picture recognition task based on which we built the old-new fMRI contrast and decomposed into 12 ICs. As this temporal order renders predicting N-Back and picture free-recall performance based on the brain activation ICs unsuitable, we instead conducted association analyses for these behaviours.

In order to identify the most relevant ICs for each behavioural measure, we applied both forward and backward stepwise model selection using the "stepAIC" function from the "MASS" R package [39]. We used this function to select the best-performing model out of 13 possible linear models with 0–12 ICs as independent variables and the respective behavioural measure as a dependent variable, separately for each sample.

2.10. Data availability

The anatomical atlas is provided in Appendix B, DataS1 and the IC voxel loadings from the training sample are provided in Appendix B, DataS2. The beta coefficients from our prediction model are reported in Table 3. Other researchers are welcome and encouraged to use these data in order to test our prediction model in additional samples. The voxel loadings for the 12 ICs are also stored online in a raw, unthresholded manner in the public repository NeuroVault [41] and can be retrieved from https://neurovault.org/collections/ITSIOTJG/.

If needed, further information and scripts for data analysis will also be available upon request.

2.11. Description and analyses of Neurosynth data

We used Neurosynth data in order to compare our results with previous research. Neurosynth (https://neurosynth.org/) is a freely available database containing large-scale meta-analyses of fMRI studies for commonly investigated terms and topics [42]. We downloaded the association test maps from the term-based automated meta-analyses for recognition memory ($N_{studies} = 148$), familiarity ($N_{studies} = 188$) and recollection ($N_{studies} = 157$), respectively. The association test maps display voxels that are reported more often in articles with abstracts containing the term than in articles with abstracts not containing it, i.e., voxels which are preferentially related to the term in questions. The association maps contain estimates for voxels with FDR-corrected ($\alpha = 0.01$) significant associations. We registered the association map for each term to the image space of our fMRI data using FLIRT [43–45].

As a general validation step for our brain activation contrast of interest, we calculated the overlap between recognition memory related brain activation in Neurosynth and brain activation related to the testing phase of our recognition memory task. First, we applied voxel-wise one-sample t tests to the parameter estimates of the old-new contrast from our own study. Based on these tests, we identified voxels with the highest (top 5 %) difference in brain activation between viewing of old vs. new pictures in either direction. Next, we calculated the percentage of Neurosynth voxels related to recognition memory, familiarity and recollection, respectively, that were also within the top 5 % of old vs. new pictures brain activation.

Furthermore, we calculated the overlap between voxels related to recognition memory, familiarity and recollection, respectively, in Neurosynth and each of our ICs. For each IC, we identified voxels with the strongest loadings (overall top 5 %) in the training sample (as depicted in Fig. 2). Next, we calculated the number of such top 5 % voxels per IC that overlap with significant Neurosynth voxels for each relevant term, separately. We also calculated the percentage of Neurosynth voxels for each relevant term that belong to the top 5 % voxels per IC.

3. Results

During the picture-recognition task, participants were shown 72 previously seen (old) and 72 new pictures and rated each of them as remembered (recollection), familiar (familiarity), or new (novelty). We analysed participants' brain activity when looking at old in comparison to new pictures (fMRI contrast old-new).

To achieve a robust estimation of networks of brain activation and of model fit when predicting the behavioural outcome, we divided the full sample into three independent samples for the following analyses (training sample: $N = 645$, replication sample: $N = 665$ and test sample: $N = 100$). Demographic characteristics per sample are presented in Table 1.

The training and replication samples were used to determine the optimal number of brain networks that can be robustly identified, whereas the test sample was used to achieve unbiased estimates for prediction accuracy.

3.1. Behavioural results

The mean overall recognition memory performance of our total sample was 61.36 (SD = 7.70), 3.53 (SD = 11.29) for familiarity and

Table 1
Demographic characteristics (sex and age), shown separately for the training, replication and test sample.

	Training sample	Replication sample	Test sample
N females (%)	412 (61.22)	406 (60.33)	75 (75)
Age range	18 - 35	18 - 34	18 - 31
Mean age	22.4	22.42	22.15

57.83 (SD = 10.77) for recollection. Descriptive statistics for recognition memory performance scores in the training, replication and test sample separately are reported in Table 2. The average number of raw hits, misses, correct rejections and false alarms per sample are reported in Suppl. Table 1. Signal Detection Theory indices (d' and c), calculated with the 'dprime' function of the psycho (v. 0.5.0) R package [46], are also reported in Suppl. Table 1. Additional information regarding the contribution of old and new picture ratings to the familiarity and recollection scores and ceiling effects is provided in the first paragraph of the Supplementary Material and Suppl. Fig. 1.

Recognition memory performance was significantly associated with participants' sex and age in the total sample (sex: $M_{female} = 61.76$, $M_{male} = 60.72$, $t_{(1'056.7)} = 2.42$, $p = 0.016$; age: $t_{(1'408)} = -2.55$, $p = 0.011$). Familiarity-based memory performance was also significantly associated with sex and age ($sex_{familiarity}$: $M_{female} = 4.23$, $M_{male} = 2.40$, $t_{(1'096.4)} = 2.94$, $p = 0.003$; $age_{familiarity}$: $t_{(1'408)} = -2.90$, $p = 0.004$; $sex_{recollection}$: $M_{female} = 57.53$, $M_{male} = 58.32$, $t_{(1'095.4)} = 1.32$, $p = 0.186$; $age_{recollection}$: $t_{(1'408)} = 1.22$, $p = 0.223$). Therefore, all subsequent analyses using behavioural data were corrected for sex and age.

3.2. fMRI old-new contrast result

We applied voxel-wise ($N = 56'764$ voxels) one-sample *t*-tests to the parameter estimates of the old-new contrast in our overall sample. Due to our large sample size, brain activation within the majority of voxels ($N = 49'157$) significantly differed ($p < 0.05$, FDR-corrected) between viewing of old vs. new pictures. Therefore, in order to depict the most relevant brain areas for this contrast, we focused on the voxels with the top 5 % of old-new contrast parameter statistics (*t*-values), including both positive and negative values (Fig. 1 A). These voxels were located predominantly in occipital regions, left lateralized frontal regions and bilateral parietal regions (Suppl. Table 2).

Next, we compared our old-new contrast parameters with external recognition memory-related fMRI data from the Neurosynth database. Despite the wide variability of studies included in the Neurosynth meta-analysis, 21 % of recognition memory-related voxels in Neurosynth (FDR-corrected, $\alpha = 0.01$) also had the highest difference (top 5 %) in brain activation between old and new pictures in our study. These overlapping voxels were predominantly localized in the inferior parietal lobe, the precuneus and rostral middle and superior frontal regions (Fig. 1 A and B; Suppl. Table 3). This was also the case for 13 % of familiarity-related voxels, mainly located in the inferior parietal lobe, and 14 % of voxels related to recollection, mostly located in the caudal middle frontal region, the inferior parietal region and the precuneus (Fig. 1 C and D; Suppl. Table 3).

In the old-new contrast, the parameter estimates of 22'848 voxels were significantly associated with sex and of 2'986 voxels with age ($p < 0.05$, FDR-corrected). The anatomical localization of the significant associations for sex and age is reported in Suppl. Fig. 2. Therefore, all subsequent analyses using fMRI data were corrected for sex and age.

3.3. Identification of stable and reproducible brain networks by using ICA decomposition

In order to reduce the dimensionality of the old-new fMRI contrast estimates into a set of brain networks we conducted ICA. ICA is an unbiased, data-driven method which reduces the dimensionality of the data to a lower number of statistically independent components (ICs, also termed brain networks throughout the following text) [35]. We determined the optimal number of ICs using a resampling procedure in the training sample and using independent validation in the replication sample. Specifically, we randomly selected 90 % of the participants from the training sample 100 times and repeatedly performed IC decomposition with a varying number of ICs (26 different ICA solutions: ICA_3 … ICA_{32}, see Method section). The stability per number of ICs is depicted in Fig. 2A. For each of the 5 most stable solutions (5, 10, 12, 14 and 15 ICs) we then performed IC decomposition in the entire training and the entire replication sample, respectively. The training and replication sample were of similar sample size (training $N = 645$; replication $N = 665$), which ensured comparable power in both samples for the estimation of the ICs. Based on the similarity of the voxel loadings between training and replication sample we determined the number of ICs that could be successfully replicated in an independent sample. We quantified the reproducibility per ICA solution as the average similarity (r^2 between voxel loadings) of matched vs. unmatched ICs between the training and the replication sample (see Method section), resulting in a reproducibility of 0.69, 0.47, 0.70, 0.58 and 0.54, for ICA_5, ICA_{10}, ICA_{12}, ICA_{14} and ICA_{15}, respectively (Suppl. Fig. 3 and 4). As the solution comprising 12 ICs was most accurately reproduced in the replication sample (Fig. 2B), we used this IC decomposition for the subsequent analyses. For the anatomical annotation of the 12 ICs see Fig. 3, Table 3, Suppl. Table 4 and Suppl. Fig. 5. How anatomical labelling was conducted is described in the Supplementary Material, sections 5 and 6.

Of note, the solution comprising 5 ICs (ICA_5) had comparable reproducibility and may also be a suitable candidate for downstream analyses. While we opted for the top-performing and more elaborate 12 ICs solution for our main downstream analyses, we also used ICA_5 (Suppl. Fig. 6) in additional analyses for comparison. The relationship between the 12 ICs and 5 ICs solution is presented in Suppl. Fig. 7.

3.4. Prediction of recognition memory performance based on brain activation

We investigated if we could predict a participant's recognition memory performance based on the brain activation strength in these 12 ICs. Since the ICs represent co-activation networks resulting from the decomposition of the old-new contrast, the participants' brain activation strength per IC shows the contribution of each participant to the group-level network. In the training sample, we built a linear model (LM) including the recognition memory performance scores as outcome variable and the participants' activation of the 12 ICs as predictors. A significant regression equation was found ($F_{(12,\ 632)} = 15.65$, $p < 2.2 \times 10^{-16}$, $R^2 = 0.229$, $R^2_{Adjusted} = 0.214$). We then applied the beta weights from this model (Table 3) to the brain activation of the 12 ICs in the replication sample. With this procedure, we could successfully predict recognition memory performance with significant accuracy ($r = 0.47$, $p < 2.2 \times 10^{-16}$; Fig. 4A). Importantly, in this analysis the ICs activation was independently estimated in the two samples (Table 4).

While having an independent estimation of ICs activation in the replication sample provides a robust estimate of our prediction model, it does not allow for the prediction model to be applied to a single participant. In order to assess if our prediction model can also be applied at single-participant level, we conducted an additional analysis. Specifically, we projected the voxel loadings from the ICs derived from the larger training sample ($N = 645$) onto the fMRI data of the smaller test sample ($N = 100$). We then applied the beta weights of the training sample onto these projected ICs to predict the memory performance in the test sample. Again, we were able to predict the memory performance with significant accuracy ($r = 0.50$, $p = 1.29 \times 10^{-07}$; Fig. 4 B).

The following four axis showed the strongest single-axis associations with recognition memory performance (Fig. 3, Table 3, Suppl. Table 4): IC3, which is a predominantly left frontal-parietal network; IC4, which is

Table 2
Descriptive statistics (mean and standard deviation) of recognition memory performance scores, shown separately for the training, replication and test sample.

	Training sample	Replication sample	Test sample
Recognition memory	61.59 (7.12)	61.01 (8.35)	62.20 (6.65)
Familiarity	4.26 (10.84)	2.96 (11.92)	2.57 (9.44)
Recollection	57.33 (10.89)	58.05 (10.85)	59.63 (9.22)

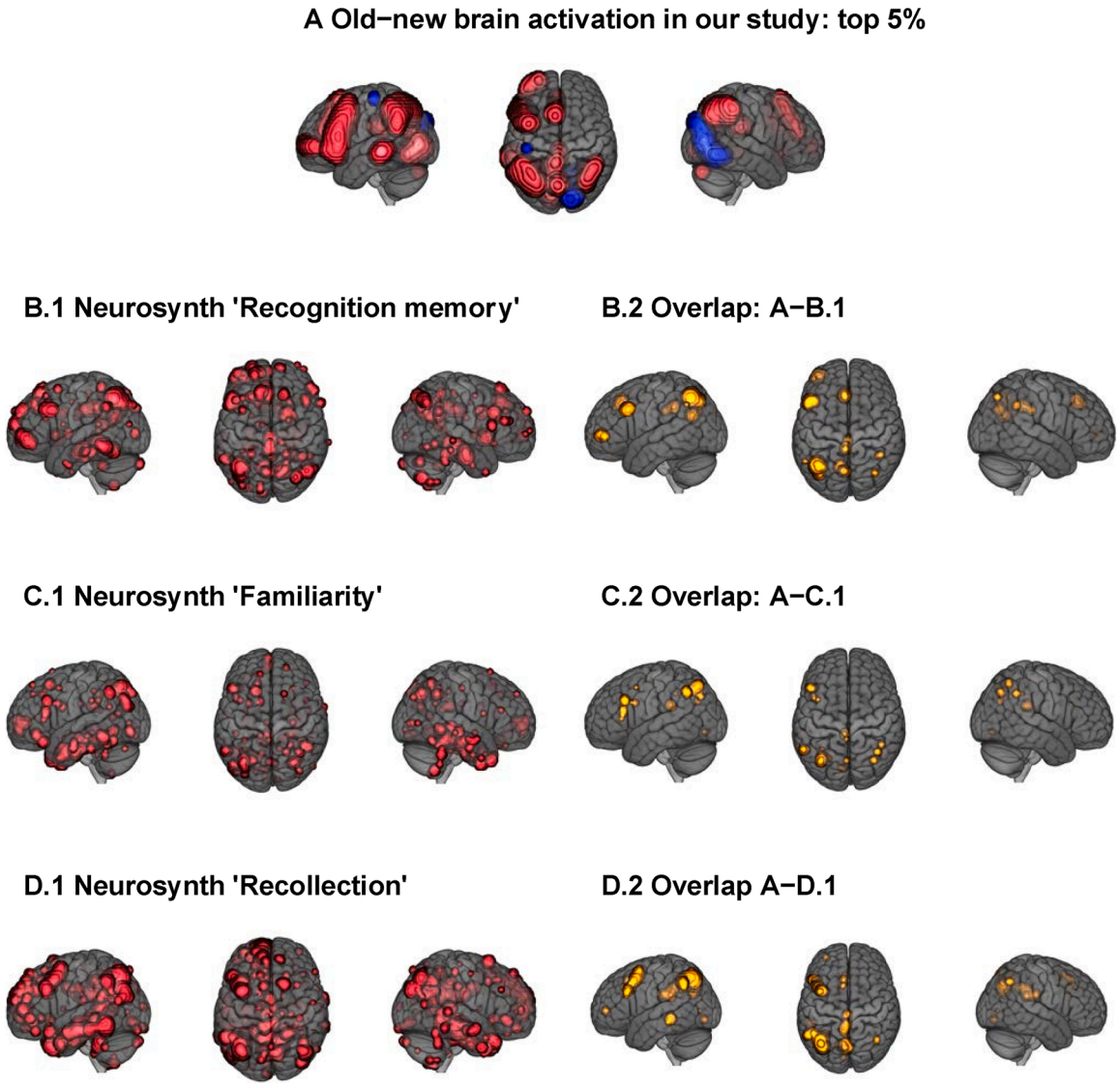

Fig. 1. A) Voxels with the highest difference in activation between viewing of old in comparison to new pictures in our sample (old-new contrast, one-sample *t*-tests, top 5 % of absolute *t*-values). Positive and negative values are presented in red and blue, respectively; Meta-analytic results retrieved from Neurosynth (association map, $\alpha = 0.01$, FDR-corrected) for the term B.1) recognition memory, C.1) familiarity and D.1) recollection. Voxels with significant Neurosynth association that also have the highest difference (top 5 %) in brain activation between old and new pictures in our own study, i.e., overlapping voxels, are presented for the term B.2) recognition memory, C.2) familiarity and D.2) recollection in yellow colour.

a right-lateralized occipital network; IC8, which is a left-lateralized occipital network; IC2 that comprises the temporal lobe and subcortical structures such as the Hippocampus and the Amygdala.

The prediction results using 5 ICs instead of 12 ICs are reported in Suppl. Table 5 and Suppl. Table 6. The 5 IC-solution provides a comparable prediction accuracy (replication sample: $r = 0.41$, $p < 2.2 \times 10^{-16}$; test sample: $r = 0.52$, $p = 2.69 \times 10^{-08}$). When comparing the 5 ICs with the 12 ICs we see a high overlap between IC3 from the 12 ICs and IC2 from the 5 ICs (58.9 %, see Suppl. Fig. 7.B). These two axes both show the strongest association with recognition memory performance (see Table 3 and Supp. Table 6). Therefore, the most relevant component for the recognition memory prediction model seems to be, at least in part, conserved between these two ICA solutions, and consistently resembles a predominantly left frontal-parietal network (Fig. 3, Table 3, Suppl. Fig. 5, Suppl. Fig. 6, Suppl. Table 4).

3.5. Prediction of familiarity and recollection separately based on brain activation

Familiarity-based and recollection-based recognition memory are often considered as separate constructs [1,4]. Therefore, we repeated the prediction analyses for familiarity-based and recollection-based recognition memory, separately, using the identical procedure, i.e., building a linear model based on the same 12 brain activation components from the old-new contrast. A significant regression equation was found for familiarity ($F_{(12,\ 632)} = 42.53$, $p < 2.2 \times 10^{-16}$, $R^2 = 0.447$, $R^2_{Adjusted} = 0.436$) and for recollection ($F_{(12,\ 632)} = 21.8$, $p < 2.2 \times 10^{-16}$, $R^2 = 0.293$, $R^2_{Adjusted} = 0.279$). The beta coefficients from the prediction models for familiarity and recollection are presented in Table 3. We were able to predict both familiarity and recollection with high accuracy (replication sample: familiarity: $r = 0.69$, $p < 2.2 \times 10^{-16}$, recollection: $r = 0.50$, $p < 2.2 \times 10^{-16}$; test sample: familiarity: $r = 0.68$, $p = 1.02 \times 10^{-14}$, recollection: $r = 0.45$, $p = 2.48 \times 10^{-06}$, Suppl. Fig. 8).

Of note, IC2 that comprises the temporal lobe and subcortical structures such as the Hippocampus and the Amygdala is significantly

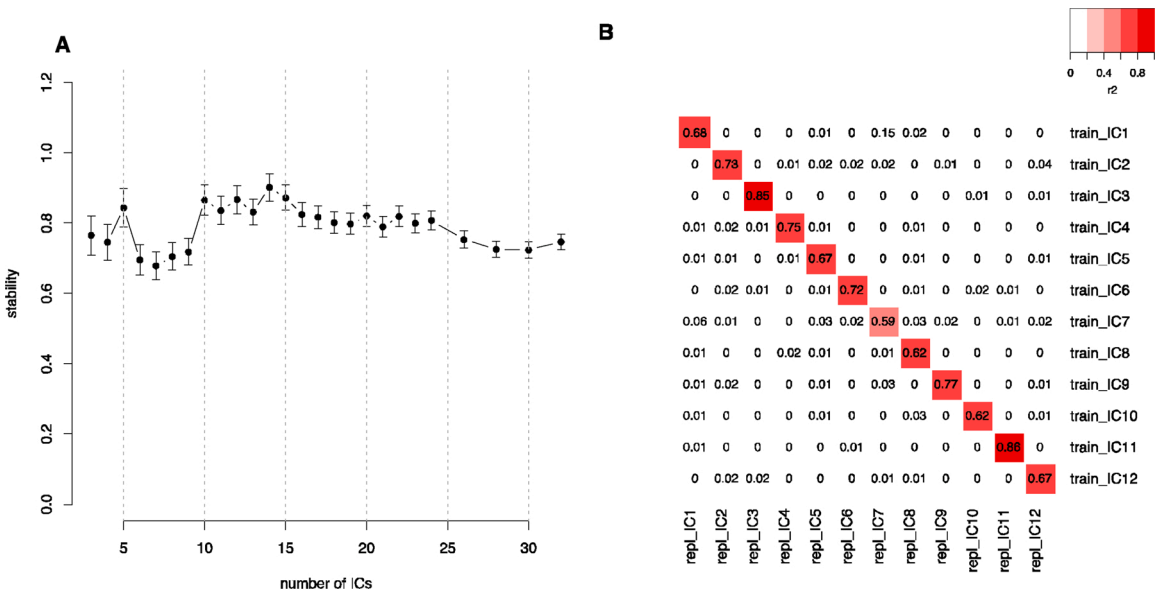

Fig. 2. ICA stability and reproducibility. A) Stability (y-axis) calculated as the mean correlation (r^2) of voxel loadings across 100 runs from the resampling procedure, averaged across ICs. This was done separately for different number of ICs (x-axis). The error bars represent 90 % confidence intervals. B) Reproducibility, i.e., correlation (r^2) between voxel loadings in the training sample and the replication sample, of the IC solution with 12 ICs. Abbreviations: train, training sample; repl, replication sample, IC, independent component.

associated with recognition memory performance and recollection, but not familiarity (Table 3). Right frontoparietal (IC9) and bilateral frontal (IC7) ICs have high contribution to the prediction of interindividual differences in both familiarity and recollection performance, however with reversed signs. Therefore, they are not associated with the general recognition memory prediction model. IC3, the predominantly left frontal-parietal network, appears to contribute more to familiarity and IC4, the predominantly right-lateralized occipital IC, more to recollection. IC3 and IC4 also have high contribution to the general recognition memory estimation. IC6 (mainly cerebellum) has higher contribution to the prediction model for familiarity than for recollection, while the opposite is the case for IC8 (left-lateralized occipital regions).

Familiarity and recollection scores were negatively correlated (r = -0.76, $p < 2.2 \times 10^{-16}$) in the overall sample. Since the behavioural outcomes show a high negative correlation, it was also possible to derive familiarity using the beta coefficients from the recollection-based model (replication sample: r = -0.61, $p < 2.2 \times 10^{-16}$; test sample: r = -0.58, $p = 1.65 \times 10^{-10}$) and recollection using the beta coefficients from the familiarity-based model (replication sample: r = -0.46, $p < 2.2 \times 10^{-16}$; test sample: r = -0.43, $p = 6.19 \times 10^{-06}$, Suppl. Fig. 9), however with reversed signs.

3.6. Post hoc analyses

3.6.1. Reduction of the prediction model

Next, we investigated if an equally high prediction of the behavioural measures can be achieved by using only the ICs which have the highest contribution to behaviour, rather than all 12 ICs. Using both forward and backward model selection in the training sample, we established that the best model fit was achieved when using 8 ICs (ICs numbered 1:4, 6:9) for recognition memory ($F_{(8, 636)} = 23.07$, $p < 2.2 \times 10^{-16}$, $R^2 = 0.225$, $R^2_{Adjusted} = 0.215$), 9 ICs (ICs numbered 3, 5:12) for familiarity ($F_{(9, 635)} = 56.71$, $p = 2.2 \times 10^{-16}$, $R^2 = 0.446$, $R^2_{Adjusted} = 0.438$) and all 12 ICs for recollection ($F_{(12, 632)} = 21.8$, $p < 2.2 \times 10^{-16}$, $R^2 = 0.293$, $R^2_{Adjusted} = 0.279$). Next, we used the best-fitting model in order to predict recognition memory and familiarity in the replication and the test sample, respectively. As the best-fitting model for recollection included all 12 ICs, a reduced model prediction was not performed for this behavioural measure. We were able to predict both the overall recognition memory and familiarity with high accuracy based on their respective best-fit models (replication sample: recognition memory: $r = 0.48$, $p < 2.2 \times 10^{-16}$, familiarity: $r = 0.69$, $p < 2.2 \times 10^{-16}$; test sample: recognition memory: $r = 0.54$, $p = 7.92 \times 10^{-09}$, familiarity: $r = 0.68$, $p = 9.52 \times 10^{-15}$). Of note, the prediction accuracy estimates of the best-fit models are as high as the estimates from the full models including all 12 ICs. Beta coefficients and p-values from the reduced linear models are reported in Table 5.

3.6.2. Association results for additional behavioural tasks

Next, we investigated if the old-new fMRI signal decomposed in 12 ICs is associated with additional memory-related behavioural measures. We built two separate linear models including participants' activation of the 12 ICs as independent variables and A) the number of freely recalled images outside of the MRI scanner and B) the D-prime 2-Back measure from the N-Back task as the outcome variable, respectively, in each sample.

3.6.2.1. Picture free-recall. A significant regression equation was found in the training and the replication sample when applying the linear model with all 12 ICs as independent variables (training sample: $F_{(12, 632)} = 8.8$, $p = 1.1 \times 10^{-15}$, $R^2 = 0.143$, $R^2_{Adjusted} = 0.127$; replication sample: $F_{(12, 652)} = 7.7$, $p = 1.8 \times 10^{-13}$, $R^2 = 0.124$, $R^2_{Adjusted} = 0.108$; test sample: $F_{(12, 87)} = 1.35$, $p = 0.207$, $R^2 = 0.157$, $R^2_{Adjusted} = 0.04$). Beta coefficients and p-values from the linear model for each sample are reported in Supplementary Table 8. Next, we investigated if a reduced model would produce comparable results in these samples. The best-performing model from the step-wise regression included 5 ICs (ICs numbered 1, 4, 5, 7, 8) in the training sample ($F_{(5, 639)} = 20$, $p < 2.2 \times 10^{-16}$, $R^2 = 0.135$, $R^2_{Adjusted} = 0.129$) and 6 ICs (ICs numbered 1, 3, 4, 8, 9, 10) in the replication sample ($F_{(6, 658)} = 14.9$, $p = 5.2 \times 10^{-16}$, $R^2 = 0.120$, $R^2_{Adjusted} = 0.112$). Beta coefficients and p-values from the reduced linear models are reported in Supplementary Table 9. In both samples the reduced models showed similar performance in comparison to the models based on all 12 ICs.

Of note, IC1 and IC4 highly contributed to the picture free-recall association model in both samples. IC4 also had high contribution to the prediction model for recognition memory, and higher contribution to the recollection-specific, than to the familiarity-specific prediction.

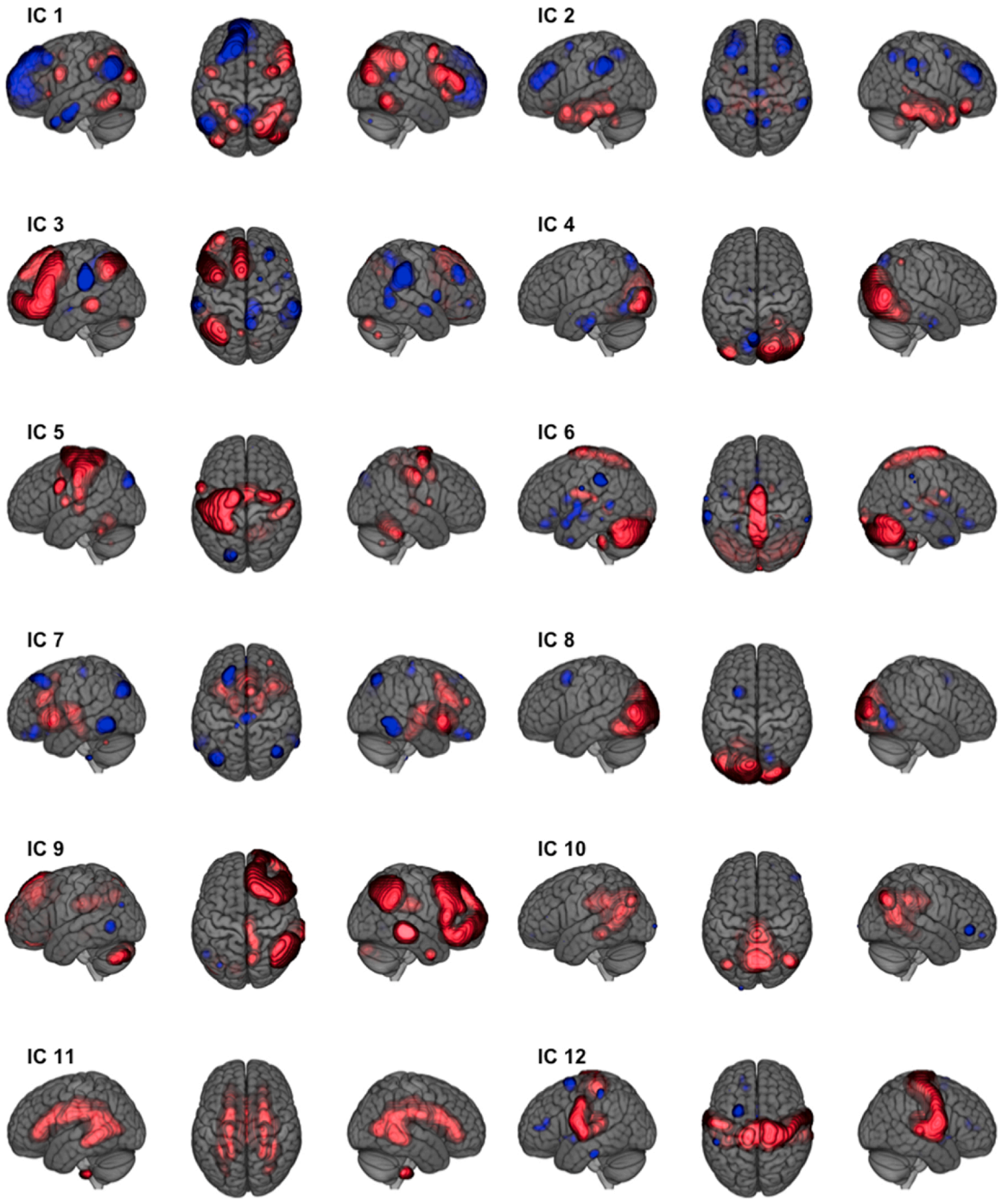

Fig. 3. Anatomical localization of the voxel loadings for each of the 12 ICs in the training sample. Only voxels with the strongest loadings (overall top 5 %) in the training sample are depicted. Positive and negative voxels loadings are presented in red and blue, respectively.

The association with free-recall performance further supports the relevance of this IC for the recollection memory process.

3.6.2.2. N-Back. A significant regression equation was found in the training and the replication sample when applying the linear model with all 12 ICs as independent variables (training sample: $F_{(12,\ 632)} = 2.45$, $p = 0.004$, $R^2 = 0.044$, $R^2_{Adjusted} = 0.026$; replication sample: $F_{(12,\ 652)} = 2.87$, $p = 0.0007$, $R^2 = 0.05$, $R^2_{Adjusted} = 0.033$; test sample: $F_{(12,\ 87)} = 1.03$, $p = 0.426$, $R^2 = 0.125$, $R^2_{Adjusted} = 0.004$). Beta coefficients and *p*-values from the linear model for each sample are reported in Supplementary Table 10. Next, we investigated if comparable results can be obtained by reduced models in these samples. The best-performing model from the step-wise regression included 4 ICs (ICs numbered 2, 3, 6 and 10) in the training sample ($F_{(4,\ 640)} = 6.45$, $p = 4.33 \times 10^{-05}$, $R^2 = 0.039$, $R^2_{Adjusted} = 0.033$) and 2 ICs (ICs numbered 1 and 3) in the replication sample ($F_{(2,\ 662)} = 16.01$, $p = 1.62 \times 10^{-07}$, $R^2 = 0.046$, $R^2_{Adjusted} = 0.043$). Beta coefficients and *p*-values from the reduced linear models are reported in Supplementary Table 11. IC3 was consistently associated with the N-Back performance in both samples.

As expected, the 2-Back performance scores on the N-back task had lower association with the brain activation ICs based on the decomposed old-new fMRI contrast, compared to the picture free-recall performance scores. Nevertheless, the significant 2-Back performance association with the brain activation ICs indicates that some of these ICs may also be

Table 3
Descriptive names of the 12 ICs, assigned considering the majority of brain regions with sizable coverage (> 10 %) per IC (see also Supplementary Table 4).

IC	IC description	IC regions
1	Bilateral fronto-parietal	Rostral anterior cingulate, Pars opercularis, Inferior and superior parietal, Caudal middle frontal, Inferior temporal, Pars triangularis
2	Temporal and subcortical	Amygdala, Hippocampus, Parahippocampal, Fusiform, Entorhinal, Ventral Diencephalon, Rostral middle frontal, Supramarginal, Temporal pole
3	Left frontal-parietal	Caudal and rostral middle frontal, Pars opercularis, Pars orbitalis, Pars triangularis, Superior frontal, Lateral orbitofrontal, Supramarginal, Inferior parietal
4	Right occipital	Pericalcarine, Cuneus, Lateral occipital, Lingual, Fusiform, Superior parietal
5	Sensorimotor 1	Precentral, Postcentral, Superior frontal, Superior parietal, Supramarginal
6	Cerebellum	Cerebellum cortex, Corpus Callosum, Lingual, Fusiform
7	Bilateral frontal	Caudal anterior cingulate, Pars opercularis, Pars triangularis
8	Left occipital	Cuneus, Lateral occipital, Lingual, Pericalcarine, Fusiform, Superior parietal
9	Right frontoparietal	Caudal middle frontal, Pars orbitalis, Rostral middle frontal, Superior frontal, Inferior parietal, Middle temporal, Pars opercularis
10	Cuneus und Precuneus	Isthmus and posterior cingulate, Corpus Callosum, Cuneus, Precuneus, Lingual
11	Corpus callosum	Caudate and Corpus Callosum
12	Sensorimotor 2	Precentral, Paracentral, Insula, Postcentral, Transverse temporal, Putamen, Superior temporal, Supramarginal

relevant in the context of a working memory task.

3.7. Neurosynth meta-analyses results overlap with voxel loadings per IC from our study

Next, we looked into the overlap between brain activation predictive of recognition memory in our study and Neurosynth recognition memory meta-analysis results, in order to estimate the comparability of our data to previous studies. Specifically, we investigated whether the ICs with highest contribution to the predictive models in our sample have substantial overlap with recognition memory, familiarity and recollection related brain activation in Neurosynth. 24 % of all voxels significantly associated with the term recognition memory in Neurosynth had very high loadings (overall top 5 %) for IC3 from our study (Fig. 5). IC3 was the component with the highest contribution to the prediction model for recognition memory performance (Table 3). No other IC contained > 20 % of voxels associated with recognition memory, familiarity or recollection in Neurosynth. A few other ICs contained > 10 % of voxels related to one of the relevant Neurosynth terms. The overlap between Neurosynth voxels related to recognition memory, familiarity and recollection, respectively, and each of our 12 ICs is presented in Suppl. Table 7 and Suppl. Fig. 10.

4. Discussion

The aim of the current study was to estimate the recognition memory performance of healthy young individuals based on a restricted set of robust brain networks summarizing their fMRI activation. Therefore, we analysed the fMRI signal of a picture-recognition memory task and deconstructed the task-based contrast "old – new pictures" into 12 brain networks using ICA. Importantly, we confirmed the robustness of this IC

Table 4
Beta coefficients and *p*-values from the linear model with memory performance scores as the outcome and the 12 brain activation ICs as predictors in the training sample.

	Recognition memory		Familiarity		Recollection	
	β	p-val	β	p-val	β	p-val
Intercept	0	1	0	1	0	1
IC1	−0.127	0.0009	−0.016	0.628	−0.068	0.064
IC2	−0.145	0.0001	0.035	0.276	−0.129	0.0003
IC3	−0.294	3.74×10^{-11}	−0.309	4.80×10^{-16}	0.112	0.007
IC4	−0.234	4.53×10^{-10}	−0.007	0.820	−0.146	4.12×10^{-05}
IC5	0.060	0.143	−0.158	7.25×10^{-06}	0.196	9.19×10^{-7}
IC6	0.100	0.006	0.145	3.20×10^{-06}	−0.078	0.026
IC7	−0.065	0.073	−0.318	$< 2 \times 10^{-16}$	0.272	1.93×10^{-14}
IC8	0.156	2.82×10^{-5}	−0.108	0.0006	0.209	5.7×10^{-09}
IC9	0.063	0.123	0.220	4.04×10^{-10}	−0.176	8.18×10^{-06}
IC10	−0.025	0.482	−0.107	0.0005	0.089	0.010
IC11	−0.032	0.380	0.094	0.002	−0.114	0.001
IC12	0.041	0.393	−0.055	0.171	0.081	0.075

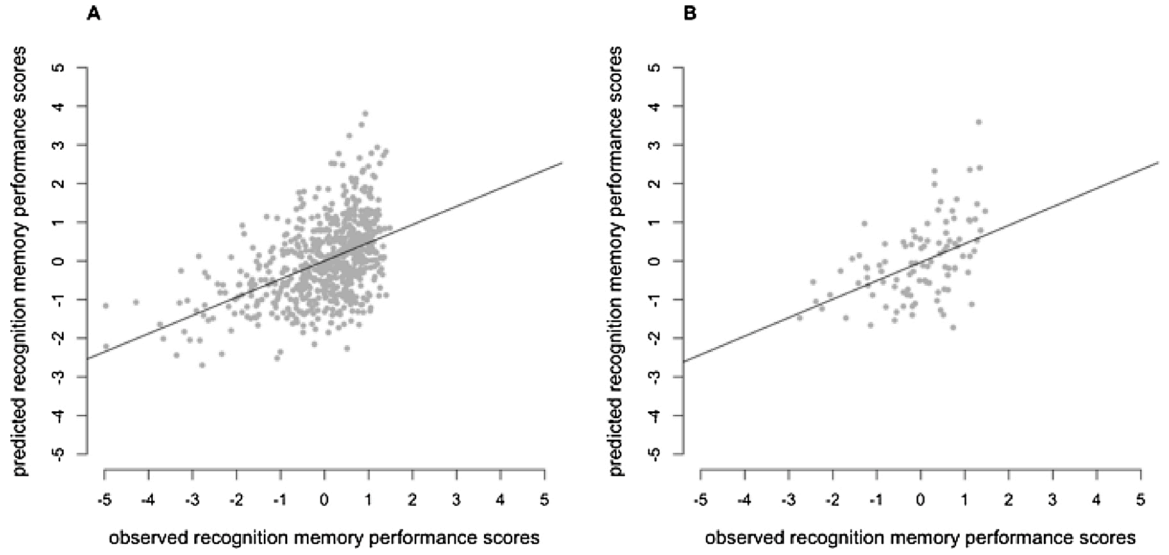

Fig. 4. Scatter plot depicting the observed and predicted recognition memory performance scores in A) the replication and B) the test sample. The figure contains scaled behavioural data.

Table 5
Beta coefficients and *p*-values from the reduced linear model with memory performance scores as the outcome and the 8 brain activation ICs as predictors for recognition memory, 9 ICs for familiarity and 12 ICs for recollection, in the training sample.

	Recognition memory		Familiarity		Recollection	
	β	p-val	β	p-val	β	p-val
Intercept	0	1	0	1	0	1
IC1	−0.124	0.0008			−0.068	0.064
IC2	−0.142	0.0001			−0.129	0.0003
IC3	−0.291	6.43×10^{-13}	−0.315	$< 2 \times 10^{-16}$	0.112	0.007
IC4	−0.232	5.40×10^{-10}			−0.146	4.12×10^{-05}
IC5			−0.154	1.00×10^{-05}	0.196	9.19×10^{-7}
IC6	0.097	0.007	0.147	1.83×10^{-06}	−0.078	0.026
IC7	−0.06	0.092	−0.317	$< 2 \times 10^{-16}$	0.272	1.93×10^{-14}
IC8	0.163	1.05×10^{-5}	−0.104	0.0007	0.209	5.7×10^{-09}
IC9	0.062	0.103	0.215	2.69×10^{-10}	−0.176	8.18×10^{-06}
IC10			−0.108	0.0003	0.089	0.010
IC11			0.096	0.002	−0.114	0.001
IC12			−0.063	0.109	0.081	0.075

estimation by using an independent replication sample. Based on the activation in these 12 brain networks we could predict recognition memory performance in a third independent sample. These results reveal the close relationship between the fMRI activation pattern when processing old compared to new pictures and the corresponding memory-related behavioural outcome.

Focusing on few robust networks and their relation to the behavioural outcome improves data reproducibility and interpretability, which is important especially in the context of basic clinical-related research [47,48]. Given the stability of the IC estimation confirmed in two independent samples and the prediction accuracy estimated in a third independent sample, the identified network-level brain activation may be considered as potential imaging biomarker of recognition memory performance in healthy young adults.

Of note, our training, replication and test samples were derived from the same single-centre study population, avoiding potential noise due to differences in sample and study characteristics. However, the results remain to be externally validated, in order to further assess the generalizability of our findings. For example, one can investigate if the estimation of our model can be generalized to brain activation data obtained by a different scanner, while performing a comparable, but not identical task, in samples with different demographic characteristics or in clinical samples. Importantly, the brain-level data per network and the predictive model are freely available for further investigation.

Brain imaging-derived predictive models typically focus on identifying biomarkers of diagnostic categories. However, it has been suggested that investigating mental processes which are variously altered in

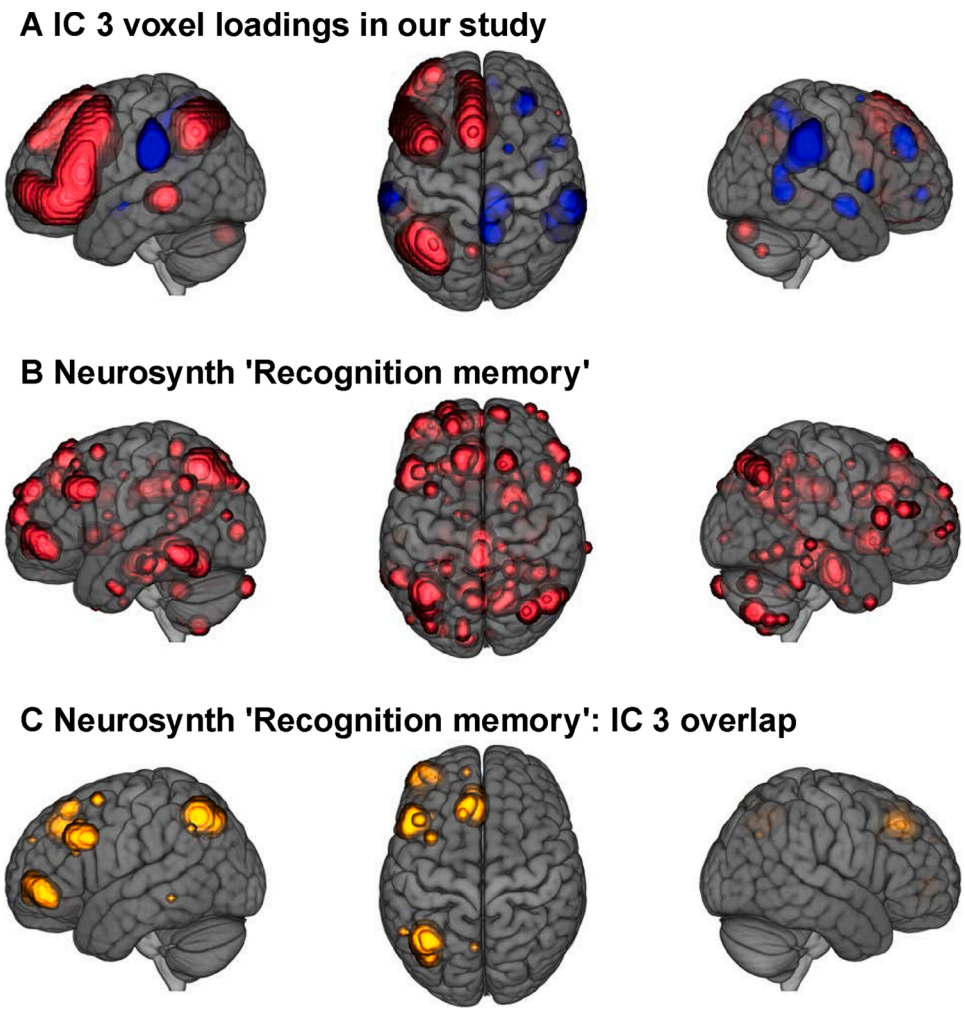

Fig. 5. A) Anatomical localization of the voxel loadings for IC3 in the training sample. Only voxels with the strongest loadings (overall top 5 %) in the training sample are depicted. Positive and negative voxels loadings are presented in red and blue, respectively. B) Meta-analytic results for the term *recognition memory* retrieved from Neurosynth (NSRM), association map, FDR corrected, $\alpha = 0.01$. C) NSRM voxels that also have high loadings (overall top 5 %) in IC3 from our training sample, i.e., overlapping voxels.

different states and disorders may produce more accurate biomarkers, as they are less restricted by theoretical constructs and assumptions [49,50]. Recognition memory is a mental process which has an important role in our everyday life and aids efficient decision making [3]. Deficits in recognition memory performance have been associated with healthy aging, mild cognitive impairment and Alzheimer's disease, as well as schizophrenia [5,6,51]. While we conducted basic research on interindividual differences in healthy young individuals in this study, the identified networks have potential relevance in the context of both neuronal processes in healthy individuals and neuropathology. For example, it would be interesting to see if the performance of our model significantly decreases in certain clinical populations due to distinct variability in their brain activation patterns.

However, it is important to keep in mind that in this study brain activation was recorded during the testing phase of the memory task and then used to estimate the performance on the same task. Therefore, our model may not have predictive utility per se. Nevertheless, as the 12 network-based brain activation was so closely linked to the interindividual differences in task performance, these networks can be used to gain further insight into the neurobiological underpinnings of recognition memory performance. While the nature and the neural features of recognition memory have been the object of extensive scientific research and debate [4,9], studies on the neural underpinnings of this ability typically investigate the general neural mechanisms associated with recognition memory processes [10–18] (but also see [19]). Our study focused on brain activation underlying interindividual differences in recognition memory performance.

We also investigated the compatibility of the brain activation patterns used in our study with previous fMRI contrast-based research on recognition memory processes. We used the database Neurosynth for a systematic overview of the results of such studies. 21 % of significant voxels identified in a large Neurosynth meta-analysis of diverse fMRI studies using the term "recognition memory" were located within the brain areas with the largest (top 5 %) difference in activation when looking at old vs. new pictures in our study, including the inferior parietal lobe, the precuneus and rostral middle and superior frontal regions. Importantly, this overlap with previous studies was noted even though no information regarding participants' task performance was included when building the old-new contrast. Furthermore, even a higher percentage (24 %) of all significant Neurosynth "recognition memory" voxels were located within brain areas highly loading onto a single network identified in our study (IC3). As IC3 had the highest contribution to the prediction model of recognition memory performance, this Neurosynth finding is in line with our prediction results and further emphasizes the relevance of this network in the context of recognition memory task performance. IC3 is a predominantly left frontal-parietal network. By applying an alternative analysis estimating only 5 components, we could show the stability of this specific network. Of note, other networks with high contribution to our recognition memory prediction model (IC4, IC8) did not contain many previously found recognition memory related brain areas, and therefore may be considered as a rather novel contribution to the literature. IC4 and IC8 are predominantly occipital networks.

Furthermore, based on our 12 brain networks we could also estimate with substantial accuracy recollection-based recognition memory performance and familiarity-based recognition memory performance, when taken as separate constructs. Our models point to bilateral frontal and right frontoparietal networks (IC7, IC9) having high contribution to the prediction of interindividual differences in both familiarity and recollection performance with reversed signs. These networks had a rather low contribution to the prediction of recognition memory when no distinction between familiarity and recollection was made. Furthermore, while our prediction model points to IC3 and IC4 having the highest contribution to the recognition memory estimation, IC3 appears to contribute more to familiarity and IC4 more to recollection. IC3 is a predominantly left frontal-parietal network, whereas IC4 comprises mainly right-lateralized occipital regions. Thus, these networks may be particularly relevant for each of the specific recognition memory processes, respectively. Higher contribution to the estimation model for one recognition memory process, rather than another is also seen for other networks, such as IC6 (mainly cerebellum; familiarity) and IC8 (a left-lateralized occipital network; familiarity). IC2, that comprises the temporal lobe and subcortical structures such as the Hippocampus and the Amygdala, was associated with the overall recognition memory performance and recollection but not familiarity. Of note, we did not find a striking overlap between networks with high contribution to the predictive model and the corresponding Neurosynth meta-analysis term associations for familiarity and recollection, respectively. This may be due to high variability of studies associated with these Neurosynth terms. In summary, while our prediction results are consistent between familiarity, recollection and overall recognition memory performance, the extent to which some of the networks contribute to the predictive model seems to vary between the different recognition memory measurements.

In order to further investigate the functional specificity of our brain networks, we also tested if they are related to interindividual differences in the performance of other behavioural tasks. The overall activation in these networks was associated with the performance of picture free-recall (about 12 % variance explained) and, to a lesser extent, a N-Back task (about 3 % variance explained), both conducted prior to the recognition memory task. Therefore, at least some of the here identified networks may also be relevant for other memory and cognitive processes.

Of note, one of the networks with the highest contribution to recognition memory prediction, namely IC4, also highly contributed to the picture free-recall association. This mainly right occipital network also had a high contribution to the prediction of recollection, but not familiarity, further supporting its predominant involvement in recollection-based memory. Compared to the medial temporal lobe [9], frontal [10,12] and parietal regions [12,13,17], occipital regions are less commonly mentioned in contrast-based fMRI studies of recognition memory processes using the R-K paradigm. However, previous R-K studies have shown that recollection, presumably due to its context-depended nature, can be associated with activation of content-specific sensory brain areas, including fusiform regions [15,52–54]. Furthermore, higher connectivity in the visual cortex has been related to successful memory retrieval [26]. The predominantly recollection-related IC4 in our study may be in line with these findings, as it includes brain activation within regions known to be involved in visual processing, such as the lateral occipital cortex and the fusiform area [55,56]. Of note, the one network with higher contribution to the recognition memory model than IC4 in our study, namely IC3, consisted of frontal and parietal regions. While most of these regions have been previously listed in studies including the R-K paradigm, some of them, such as superior frontal and inferior parietal regions, have been previously mentioned as more relevant for recollection, rather than familiarity [15,17]. This is not in line with our IC3 finding, as this network had higher familiarity, rather than recollection contribution and did not have a striking contribution to the picture-free recall association. However, IC3 shows a significant association with working memory performance in our sample. Therefore, further investigation of this network in the context of the R-K paradigm and similar tasks is needed, in order to determine the extent to which its contribution to recognition memory performance relies on familiarity and recollection processes or even on broader cognitive ability.

5. Conclusion

We identified 12 robust functional brain networks, based on which we successfully predicted recognition memory performance in general, as well as familiarity and recollection, separately. Given the substantial accuracy estimates, the network-level brain activation may be

considered as potential biomarker of recognition memory performances in healthy young adults and can be further investigated in health and disease.

Funding

This work was funded by the University of Basel, the Swiss National Science Foundation (grants 163434, 147570 and 159740 to D.J.-F.d.Q. and A.P.) and the European Community's Seventh Framework Programme (FP7/2007–2013) under grant agreement 602450 (IMAGEMEND; grant to A.P. and D.J.-F.d.Q.). Funders had no role in study design, data collection and analysis, decision to publish or preparation of the manuscript.

Declaration of Competing Interest

The authors report no biomedical financial interest or potential conflicts of interest.

Acknowledgments

Calculations were in part performed at sciCORE scientific computing core facility at University of Basel (http://scicore.unibas.ch/). Part of the results were presented in poster form at the SfN 2019 Conference (Chicago).

Appendix A. Supplementary data

Supplementary material related to this article can be found, in the online version, at doi:https://doi.org/10.1016/j.bbr.2021.113285.

References

[1] G. Mandler, Recognizing: the judgment of previous occurrence, Psychol. Rev. 87 (1980) 252–271, https://doi.org/10.1037/0033-295X.87.3.252.
[2] D.G. Goldstein, G. Gigerenzer, Models of ecological rationality: the recognition heuristic, Psychol. Rev. 109 (2002) 75.
[3] D.W. Heck, E. Erdfelder, Linking process and measurement models of recognition-based decisions, Psychol. Rev. 124 (2017) 442.
[4] A.P. Yonelinas, The nature of recollection and familiarity: a review of 30 years of research, J. Mem. Lang. 46 (2002) 441–517.
[5] J.D. Koen, A.P. Yonelinas, The effects of healthy aging, amnestic mild cognitive impairment, and Alzheimer's disease on recollection and familiarity: a meta-analytic review, Neuropsychol. Rev. 24 (2014) 332–354.
[6] D. Schoemaker, S. Gauthier, J.C. Pruessner, Recollection and familiarity in aging individuals with mild cognitive impairment and Alzheimer's disease: a literature review, Neuropsychol. Rev. 24 (2014) 313–331.
[7] E. Tulving, Memory and consciousness, Can. Psychol. Can. 26 (1985) 1.
[8] J.M. Gardiner, Functional aspects of recollective experience, Mem. Cognit. 16 (1988) 309–313.
[9] L.R. Squire, J.T. Wixted, R.E. Clark, Recognition memory and the medial temporal lobe: a new perspective, Nat. Rev. Neurosci. 8 (2007) 872.
[10] F. Scalici, C. Caltagirone, G.A. Carlesimo, The contribution of different prefrontal cortex regions to recollection and familiarity: a review of fMRI data, Neurosci. Biobehav. Rev. 83 (2017) 240–251, https://doi.org/10.1016/j.neubiorev.2017.10.017.
[11] G.A. Carlesimo, M.G. Lombardi, C. Caltagirone, F. Barban, Recollection and familiarity in the human thalamus, Neurosci. Biobehav. Rev. 54 (2015) 18–28, https://doi.org/10.1016/j.neubiorev.2014.09.006.
[12] A.P. Yonelinas, L.J. Otten, K.N. Shaw, M.D. Rugg, Separating the brain regions involved in recollection and familiarity in recognition memory, J. Neurosci. 25 (2005) 3002–3008, https://doi.org/10.1523/JNEUROSCI.5295-04.2005.
[13] A. Frithsen, M.B. Miller, The posterior parietal cortex: comparing remember/know and source memory tests of recollection and familiarity, Neuropsychologia. 61 (2014) 31–44, https://doi.org/10.1016/j.neuropsychologia.2014.06.011.
[14] M. Horn, R. Jardri, F. D'Hondt, G. Vaiva, P. Thomas, D. Pins, The multiple neural networks of familiarity: a meta-analysis of functional imaging studies, Cogn. Affect. Behav. Neurosci. 16 (2016) 176–190, https://doi.org/10.3758/s13415-015-0392-1.
[15] E.I. Skinner, M.A. Fernandes, Neural correlates of recollection and familiarity: a review of neuroimaging and patient data, Neuropsychologia. 45 (2007) 2163–2179, https://doi.org/10.1016/j.neuropsychologia.2007.03.007.
[16] J. Spaniol, P.S.R. Davidson, A.S.N. Kim, H. Han, M. Moscovitch, C.L. Grady, Event-related fMRI studies of episodic encoding and retrieval: meta-analyses using activation likelihood estimation, Neuropsychologia. 47 (2009) 1765–1779, https://doi.org/10.1016/j.neuropsychologia.2009.02.028.
[17] K.L. Vilberg, M.D. Rugg, Memory retrieval and the parietal cortex: a review of evidence from a dual-process perspective, Neuropsychologia. 46 (2008) 1787–1799, https://doi.org/10.1016/j.neuropsychologia.2008.01.004.
[18] H. Kim, Dissociating the roles of the default-mode, dorsal, and ventral networks in episodic memory retrieval, Neuroimage 50 (2010) 1648–1657, https://doi.org/10.1016/j.neuroimage.2010.01.051.
[19] M. de Chastelaine, J.T. Mattson, T.H. Wang, B.E. Donley, M.D. Rugg, The neural correlates of recollection and retrieval monitoring: relationships with age and recollection performance, Neuroimage. 138 (2016) 164–175, https://doi.org/10.1016/j.neuroimage.2016.04.071.
[20] S.L. Bressler, V. Menon, Large-scale brain networks in cognition: emerging methods and principles, Trends Cogn. Sci. (Regul. Ed.) 14 (2010) 277–290, https://doi.org/10.1016/j.tics.2010.04.004.
[21] B. Misic, O. Sporns, From regions to connections and networks: new bridges between brain and behavior, Curr. Opin. Neurobiol. 40 (2016) 1–7, https://doi.org/10.1016/j.conb.2016.05.003.
[22] M.D. Fox, A.Z. Snyder, J.L. Vincent, M. Corbetta, D.C. Van Essen, M.E. Raichle, The human brain is intrinsically organized into dynamic, anticorrelated functional networks, Proc Natl Acad Sci U S A. 102 (2005) 9673, https://doi.org/10.1073/pnas.0504136102.
[23] S.M. Smith, P.T. Fox, K.L. Miller, D.C. Glahn, P.M. Fox, C.E. Mackay, N. Filippini, K. E. Watkins, R. Toro, A.R. Laird, C.F. Beckmann, Correspondence of the brain's functional architecture during activation and rest, Proc Natl Acad Sci U S A. 106 (2009) 13040–13045, https://doi.org/10.1073/pnas.0905267106.
[24] J.S. Damoiseaux, S.A.R.B. Rombouts, F. Barkhof, P. Scheltens, C.J. Stam, S. M. Smith, C.F. Beckmann, Consistent resting-state networks across healthy subjects, Proc Natl Acad Sci U S A. 103 (2006) 13848–13853, https://doi.org/10.1073/pnas.0601417103.
[25] D.R. King, M. de Chastelaine, R.L. Elward, T.H. Wang, M.D. Rugg, Recollection-related increases in functional connectivity predict individual differences in memory accuracy, J. Neurosci. 35 (2015) 1763–1772, https://doi.org/10.1523/JNEUROSCI.3219-14.2015.
[26] A.M. Schedlbauer, M.S. Copara, A.J. Watrous, A.D. Ekstrom, Multiple interacting brain areas underlie successful spatiotemporal memory retrieval in humans, Sci. Rep. 4 (2014) 1–9.
[27] T. Egli, D. Coynel, K. Spalek, M. Fastenrath, V. Freytag, A. Heck, E. Loos, B. Auschra, A. Papassotiropoulos, D.J.-F. de Quervain, A. Milnik, Identification of two distinct working memory-related brain networks in healthy young adults, ENeuro. 5 (2018), https://doi.org/10.1523/ENEURO.0222-17.2018.
[28] E. Loos, T. Egli, D. Coynel, M. Fastenrath, V. Freytag, A. Papassotiropoulos, D.J.-F. de Quervain, A. Milnik, Predicting emotional arousal and emotional memory performance from an identical brain network, NeuroImage 189 (2019) 459–467, https://doi.org/10.1016/j.neuroimage.2019.01.028.
[29] A. Fornito, B.J. Harrison, A. Zalesky, J.S. Simons, Competitive and cooperative dynamics of large-scale brain functional networks supporting recollection, Proc Natl Acad Sci U S A. 109 (2012) 12788–12793, https://doi.org/10.1073/pnas.1204185109.
[30] T. Yarkoni, J. Westfall, Choosing prediction over explanation in psychology: lessons from machine learning, Perspect. Psychol. Sci. 12 (2017) 1100–1122, https://doi.org/10.1177/1745691617693393.
[31] J.D.E. Gabrieli, S.S. Ghosh, S. Whitfield-Gabrieli, Prediction as a humanitarian and pragmatic contribution from human cognitive neuroscience, Neuron. 85 (2015) 11–26, https://doi.org/10.1016/j.neuron.2014.10.047.
[32] K. Spalek, M. Fastenrath, S. Ackermann, B. Auschra, D. Coynel, J. Frey, L. Gschwind, F. Hartmann, N. Van Der Maarel, A. Papassotiropoulos, Sex-dependent dissociation between emotional appraisal and memory: a large-scale behavioral and fMRI study, J. Neurosci. 35 (2015) 920–935.
[33] A. Heck, A. Milnik, V. Vukojevic, J. Petrovska, T. Egli, J. Singer, P. Escobar, T. Sengstag, D. Coynel, V. Freytag, Exome sequencing of healthy phenotypic extremes links TROVE2 to emotional memory and PTSD, Nat. Hum. Behav. 1 (2017) 0081.
[34] P. Lang, M. Bradley, B. Cuthbert, International Affective Picture System (IAPS): Affective Ratings of Pictures and Instruction Manual, University of Florida, Gainesville, Tech Rep A-8, 2008.
[35] A. Hyvarinen, E. Oja, Independent component analysis: algorithms and applications, Neural Netw. 13 (2000) 411–430, https://doi.org/10.1016/s0893-6080(00)00026-5.
[36] P. Chiappetta, M.-C. Roubaud, B. Torrésani, Blind source separation and the analysis of microarray data, J. Comput. Biol. 11 (2004) 1090–1109.
[37] U. Kairov, L. Cantini, A. Greco, A. Molkenov, U. Czerwinska, E. Barillot, A. Zinovyev, Determining the optimal number of independent components for reproducible transcriptomic data analysis, BMC Genomics 18 (2017) 712, https://doi.org/10.1186/s12864-017-4112-9.
[38] A.R. Franco, M.V. Mannell, V.D. Calhoun, A.R. Mayer, Impact of analysis methods on the reproducibility and reliability of resting-state networks, Brain Connect. 3 (2013) 363–374, https://doi.org/10.1089/brain.2012.0134.
[39] W.N. Venables, B.D. Ripley, Modern Applied Statistics With S, Statistics and Computing, Springer, New York, 2002.
[40] N.A. Macmillan, C.D. Creelman, Response bias: characteristics of detection theory, threshold theory, and" nonparametric" indexes, Psychol. Bull. 107 (1990) 401.
[41] K.J. Gorgolewski, G. Varoquaux, G. Rivera, Y. Schwarz, S.S. Ghosh, C. Maumet, V. V. Sochat, T.E. Nichols, R.A. Poldrack, J.-B. Poline, T. Yarkoni, D.S. Margulies, NeuroVault.org: a web-based repository for collecting and sharing unthresholded statistical maps of the human brain, Front. Neuroinform. 9 (2015) 8, https://doi.org/10.3389/fninf.2015.00008.

[42] T. Yarkoni, R.A. Poldrack, T.E. Nichols, D.C. Van Essen, T.D. Wager, Large-scale automated synthesis of human functional neuroimaging data, Nat. Methods 8 (2011) 665–670, https://doi.org/10.1038/nmeth.1635.
[43] M. Jenkinson, S. Smith, A global optimisation method for robust affine registration of brain images, Med. Image Anal. 5 (2001) 143–156, https://doi.org/10.1016/s1361-8415(01)00036-6.
[44] M. Jenkinson, P. Bannister, M. Brady, S. Smith, Improved optimization for the robust and accurate linear registration and motion correction of brain images, Neuroimage. 17 (2002) 825–841, https://doi.org/10.1016/s1053-8119(02)91132-8.
[45] D.N. Greve, B. Fischl, Accurate and robust brain image alignment using boundary-based registration, Neuroimage. 48 (2009) 63–72, https://doi.org/10.1016/j.neuroimage.2009.06.060.
[46] D. Makowski, The psycho package: an efficient and publishing-oriented workflow for psychological science, J. Open Source Softw. 3 (2018) 470.
[47] R.A. Poldrack, M.J. Farah, Progress and challenges in probing the human brain, Nature. 526 (2015) 371–379, https://doi.org/10.1038/nature15692.
[48] R.R. Darby, J. Joutsa, M.D. Fox, Network localization of heterogeneous neuroimaging findings, Brain. 142 (2019) 70–79.
[49] C.-W. Woo, L.J. Chang, M.A. Lindquist, T.D. Wager, Building better biomarkers: brain models in translational neuroimaging, Nat. Neurosci. 20 (2017) 365.
[50] M.S. Mellem, Y. Liu, H. Gonzalez, M. Kollada, W.J. Martin, P. Ahammad, Machine learning models identify multimodal measurements highly predictive of transdiagnostic symptom severity for mood, anhedonia, and anxiety, Biol. Psychiatry Cogn. Neurosci. Neuroimaging 5 (2020) 56–67, https://doi.org/10.1016/j.bpsc.2019.07.007.
[51] L.A. Libby, A.P. Yonelinas, C. Ranganath, J.D. Ragland, Recollection and familiarity in schizophrenia: a quantitative review, Biol. Psychiatry 73 (2013) 944–950.
[52] M.E. Wheeler, R.L. Buckner, Functional-anatomic correlates of remembering and knowing, NeuroImage. 21 (2004) 1337–1349, https://doi.org/10.1016/j.neuroimage.2003.11.001.
[53] D.B. Fenker, B.H. Schott, A. Richardson-Klavehn, H. Heinze, E. Düzel, Recapitulating emotional context: activity of amygdala, hippocampus and fusiform cortex during recollection and familiarity, Eur. J. Neurosci. 21 (2005) 1993–1999.
[54] C.C. Woodruff, J.D. Johnson, M.R. Uncapher, M.D. Rugg, Content-specificity of the neural correlates of recollection, Neuropsychologia. 43 (2005) 1022–1032, https://doi.org/10.1016/j.neuropsychologia.2004.10.013.
[55] Y. Lerner, B. Epshtein, S. Ullman, R. Malach, Class information predicts activation by object fragments in human object areas, J. Cogn. Neurosci. 20 (2008) 1189–1206, https://doi.org/10.1162/jocn.2008.20082.
[56] R. Malach, J.B. Reppas, R.R. Benson, K.K. Kwong, H. Jiang, W.A. Kennedy, P. J. Ledden, T.J. Brady, B.R. Rosen, R.B. Tootell, Object-related activity revealed by functional magnetic resonance imaging in human occipital cortex, Proc. Natl. Acad. Sci. U. S. A. 92 (1995) 8135–8139, https://doi.org/10.1073/pnas.92.18.8135.